Journal of Hydrology 570 (2019) 69–79

Contents lists available at ScienceDirect

Journal of Hydrology

journal homepage: www.elsevier.com/locate/jhydrol

Research papers

Isotopic evidence of nitrate degradation by a zero-valent iron permeable reactive barrier: Batch experiments and a field scale study

A. Grau-Martínez[a], C. Torrentó[a,*], R. Carrey[a], A. Soler[a], N. Otero[a,b]

[a] Grup MAiMA, Mineralogia Aplicada, Geoquímica i Geomicrobiologia, Departament de Mineralogia, Petrologia i Geologia Aplicada, SIMGEO UB-CSIC, Facultat de Ciències de la Terra, Universitat de Barcelona (UB), C/ Martí i Franquès, s/n, 08028 Barcelona, Spain
[b] Serra Hunter Fellow, Generalitat de Catalunya, Spain

ARTICLE INFO

This manuscript was handled by Huaming Guo, Editor-in-Chief, with the assistance of Jiin-Shuh Jean, Associate Editor

Keywords:
Groundwater remediation
Passive treatment system
Abiotic nitrate reduction
Denitrification
Multi-isotope analysis

ABSTRACT

Permeable reactive barriers (PRBs) filled with zero-valent iron (ZVI) are a well-known remediation approach to treat groundwater plumes of chlorinated volatile organic compounds as well as other contaminants. In field implementations of ZVI-PRBs designed to treat these contaminants, nitrate consumption has been reported and has been attributed to direct abiotic nitrate reduction by ZVI or to denitrification by autochthonous microorganisms using the dissolved hydrogen produced from ZVI corrosion. Isotope tools have proven to be useful for monitoring the performance of nitrate remediation actions. In this study, we evaluate the use of isotope tools to assess the effect of ZVI-PRBs on the nitrate fate for the further optimization of full-scale applications. Laboratory batch experiments were performed using granular cast ZVI and synthetic nitrate solutions at pH 4–5.5 or nitrate-containing groundwater (pH = 7.0) from a field site where a ZVI-PRB was installed. The experimental results revealed nitrate attenuation and ammonium production for both types of experiments. In the field site, the chemical and isotopic data demonstrated the occurrence of ZVI-induced abiotic nitrate reduction and denitrification in wells located close to the ZVI-PRB. The isotopic characterization of the laboratory experiments allowed us to monitor the efficiency of the ZVI-PRB at removing nitrate. The results show the limited effect of the barrier (nitrate reduction of less than 15–20%), probably related to its non-optimal design. Isotope tools were therefore proven to be useful tools for determining the efficacy of nitrate removal by ZVI-PRBs at the field scale.

1. Introduction

Nitrate (NO_3^-) contamination in groundwater is a common and increasing global problem that affects drinking water supplies around the world. Biological denitrification is the major nitrate removal mechanism under natural conditions. However, in many contaminated aquifers, the activity of nitrate-reducing bacteria is limited by the availability of electron donors (Rivett et al., 2008). Therefore, over the last couple of decades, various remediation techniques have been explored for groundwater clean-up (Khan et al., 2004). One of the innovative technologies used for in situ remediation of contaminated groundwater is the use of permeable reactive barriers (PRBs) (U.S. EPA, 2002; Tratnyek et al., 2003). This in situ remediation technique involves the interception of groundwater flow to remove contaminants by physical, chemical or biological processes. Several constructed PRBs filled with zero-valent iron (ZVI) have been used to treat groundwater contaminated with chlorinated volatile organic compounds (O'Hannesin and Gillham, 1998; Phillips, 2010; Wilkin et al., 2014; Audí-Miró et al., 2015), chromium (VI) (Flury et al., 2009; Wilkin et al., 2014), sulfates (Da Silva et al., 2007), pesticides (Yang et al., 2010), explosives (Da Silva et al., 2007; Johnson and Tratnyek, 2008) or radionuclides, such as uranium (Gu et al., 2002a; Morrison et al., 2002).

The success of these barriers has stimulated significant interest in the application of ZVI to other contaminants, such as nitrate. Gu et al. (2002a) observed decreases in nitrate concentrations in downgradient (and some upgradient) monitoring wells of a ZVI-PRB installed to remove the radionuclides uranium and technetium. The decrease in the nitrate content was attributed to direct abiotic nitrate reduction by ZVI or to denitrification by microorganisms that use the dissolved hydrogen produced from ZVI corrosion. Morrison et al. (2002) also observed decreases in nitrate contents in monitoring wells located in and around a ZVI-PRB installed in a former uranium milling site for the removal of uranium and vanadium. Nitrate removal has also been reported in a ZVI pilot-scale funnel-and-gate system designed to treat groundwater contaminated with trichloroethylene (Yabusaki et al., 2001). Finally, Hosseini et al. (2018) demonstrated the efficiency in nitrate removal

* Corresponding author.
E-mail address: clara.torrento@ub.edu (C. Torrentó).

https://doi.org/10.1016/j.jhydrol.2018.12.049
Received 12 September 2018; Received in revised form 21 November 2018; Accepted 13 December 2018
Available online 11 January 2019

from groundwater of non-pumping reactive wells (NPRWs) filled with a mixture of nano/micro ZVI in bench-scale laboratory tests.

At the laboratory scale, numerous studies have demonstrated the effectiveness of ZVI for the abiotic reduction of nitrate (Huang et al., 1998; Westerhoff and James, 2003; Huang and Zhang, 2004; Shin and Cha, 2008, Liu et al., 2013; Zhang et al., 2017). The following reaction pathway (Eq. (1)) has been proposed to be the dominant one during abiotic nitrate reduction by ZVI (Yang and Lee, 2005; Rodríguez-Maroto et al., 2009):

$$4Fe^0 + NO_3^- + 10H^+ \rightarrow 4Fe^{2+} + NH_4^+ + 3H_2O \quad (1)$$

Ammonium is the main product in nitrate reduction by ZVI (Huang et al., 1998; Suzuki et al., 2012), although other products, such as nitrite and nitrogen gas, have also been reported (Choe et al., 2000; Shin and Cha, 2008). The main limitation in the application of ZVI-PRB to reduce nitrate is therefore the generation of ammonium ions that are potentially toxic to aquatic organisms at high concentrations (Shin and Cha, 2008; Hwang et al., 2011; Suzuki et al., 2012). Furthermore, since nitrate is corrosive to ZVI, clogging processes may affect the performance of hydraulic PRBs (Gu et al., 2002a; Ritter et al., 2002), especially at high nitrate concentrations (Kamolpornwijit et al., 2003; Liang et al., 2005).

The combined use of ZVI and a carbon substrate for in situ biochemical denitrification has been considered in recent years and has been shown to be effective at the laboratory scale in improving denitrification rates (Della Rocca et al., 2006, 2007). Huang et al. (2015) and Hosseini and Tosco (2015) demonstrated the efficacy of nitrate removal from contaminated groundwater by a combination of ZVI and carbon substrates (pine bark, beech sawdust and maize cobs) in laboratory tests. Liu et al. (2013) demonstrated that the main role of ZVI in two-layer permeable reactive barriers consisting of ZVI and activated carbon immobilizing denitrifying microbial consortia was as an oxygen capturing reagent and not for direct nitrate reduction.

When iron metal is immersed in water under anaerobic conditions, its corrosion produces cathodic hydrogen following Eq. (2) (Reardon, 1995). This cathodic hydrogen can be used as an electron donor by autotrophic denitrifiers for nitrate reduction (Till et al., 1998) (Eq. (3)).

$$Fe^0 + 2H_2O \rightarrow H_2 + Fe^{2+} + 2OH^- \quad (2)$$

$$2NO_3^- + 5H_2 \rightarrow N_2 + 4H_2O + 2OH^- \quad (3)$$

The use of this cathodic hydrogen as an energy source to support bacterial growth has been demonstrated for several types of anaerobic pure cultures, including autotrophic denitrifiers (Till et al., 1998) and methanogenic, homoaceotogenic, and sulfate-reducing bacteria (Daniels et al., 1987; Rajagopal and LeGall, 1989). An indigenous hydrogenotrophic consortium is thus likely to eventually develop around a hydrogen-producing ZVI-PRB. Gu et al. (2002b) found that the depletion of dissolved oxygen and the production of cathodic hydrogen by ZVI corrosion in a ZVI-PRB designed for the sequestration or removal of uranium provided a reducing environment favorable to many hydrogen-consuming anaerobic microorganisms, such as sulfate and metal-reducing bacteria, methanogens, and denitrifying bacteria. Da Silva et al. (2007) also identified several bacteria that could utilize hydrogen produced during anaerobic ZVI corrosion in groundwater samples from within and around a ZVI-PRB installed for the remediation of a site contaminated with explosives. Denitrifying bacteria may therefore greatly increase the rate and extent of nitrate reduction in the reducing zone of a ZVI-PRB. The combination of ZVI-driven nitrate reduction with denitrification by autohydrogenotrophic denitrifying bacteria has been proved at the laboratory scale, resulting in an increase in the nitrate removal rate and a decrease in ammonium release (Dejournett and Alvarez, 2000; Shin and Cha, 2008; An et al., 2009).

Induced nitrate attenuation at the field scale may be masked by several processes, such as dispersion, diffusion or dilution (mixing), which can change the nitrate concentration in groundwater. The isotopic fractionation of N ($\varepsilon^{15}N$) and O ($\varepsilon^{18}O$) of dissolved nitrate calculated following a Rayleigh distillation process in lab-scale experiments of denitrification with ZVI may be used in future studies to assess the behavior of the system in the field and optimize full-scale applications. To the authors' knowledge, the oxygen and nitrogen isotopic fractionations associated with nitrate reduction by ZVI have not yet been reported in the literature. The potential use of the in situ measurement of the isotopic composition of nitrate to assess the effectiveness of ZVI-PRBs at removing nitrate has yet to be evaluated.

The main objective of this study is therefore to determine the nitrogen and oxygen isotope fractionations ($\varepsilon^{15}N$ and $\varepsilon^{18}O$) associated with the ZVI-driven nitrate reduction reaction to investigate the potential of isotope analyses to assess the fate of nitrate in a PRB-ZVI installed in a site contaminated with volatile organic compounds where high nitrate concentrations in groundwater are detected.

2. Study area

The study site is located in the industrial area of Granollers, 20 km NW of Barcelona, Catalonia. An automotive industry that used tetrachloroethene and trichloroethene as degreasers operated in the area from 1965 to 1989. Groundwater contamination by chlorinated solvents resulted from the discharge of industrial waters into a seepage pit located to the south of the plant (close to MW17 well, Fig. 1). The lithology of the site is mainly composed of an alternation of sand and silt Miocene sediments in a clay matrix that extends from 4 m to a minimum of 14 m in depth (Audí-Miró et al., 2015). Above these materials, there are 4 m of quaternary glacis formed by the Miocene materials that are mainly composed of poorly structured clays and silts. The water table of the aquifer is located at an average depth of 5.4 ± 2.1 m. The deepest water table (approximately 8 m) was measured at the base and at the top of the studied valley area (length of the studied area is 900 m). At approximately 300 m from the top of this area, the water table was located closer to the surface (approximately 3 m in depth) (Fig. 1). The average water table variation due to seasonal changes was −0.5 ± 0.9 m. The groundwater flow direction was NE to W-SW, and the flow velocity was estimated at approximately 0.16 m day^{-1} at the shallow quaternary clay depth and 0.84 m day^{-1} at the sandier Miocene depth (Audí-Miró et al., 2015). The site is crossed by the Can Ninou Creek along which a piezometer network was installed (Fig. 1).

In 2009, contaminated soil from the source area was removed, and in 2010, a ZVI-PRB was installed (Audí-Miró et al., 2015). The ZVI-PRB was built approximately 320 m downgradient of the contaminated source, transverse to the creek, from NW to SE (Fig. 1). The top of the PRB was placed 4–5 m below the ground surface, and its size is 20 m long, 5 m high and 60 cm thick, with a 3% (v/v) granular cast ZVI inside a sand matrix.

The piezometer network consists of 12 conventional wells and 5 multilevel wells. The conventional wells were installed between 2005 and 2010 along the east bank of the creek (expected direction of groundwater flow) from the source area to 900 m downgradient of the creek (Fig. 1). The wells consists of 50 mm inner diameter PVC pipes screened from 3 to 12 m depth, except MW17 and OMW5 wells, screened from 5 to 10 m and from 7 to 11 m, respectively. In March 2012, five additional wells were installed surrounding the barrier, two immediately upgradient of the PRB and three immediately downgradient. These five wells have a multilevel sampling system installed consisting of a bundle of small-diameter (5 mm outer diameter) PTFE tubes surrounding the monitoring well casing and positioned at different depths, providing the possibility to obtain several depth discrete groundwater samples from the same borehole (from 2 to 13.5 m depth, with a 0.5 m interval).

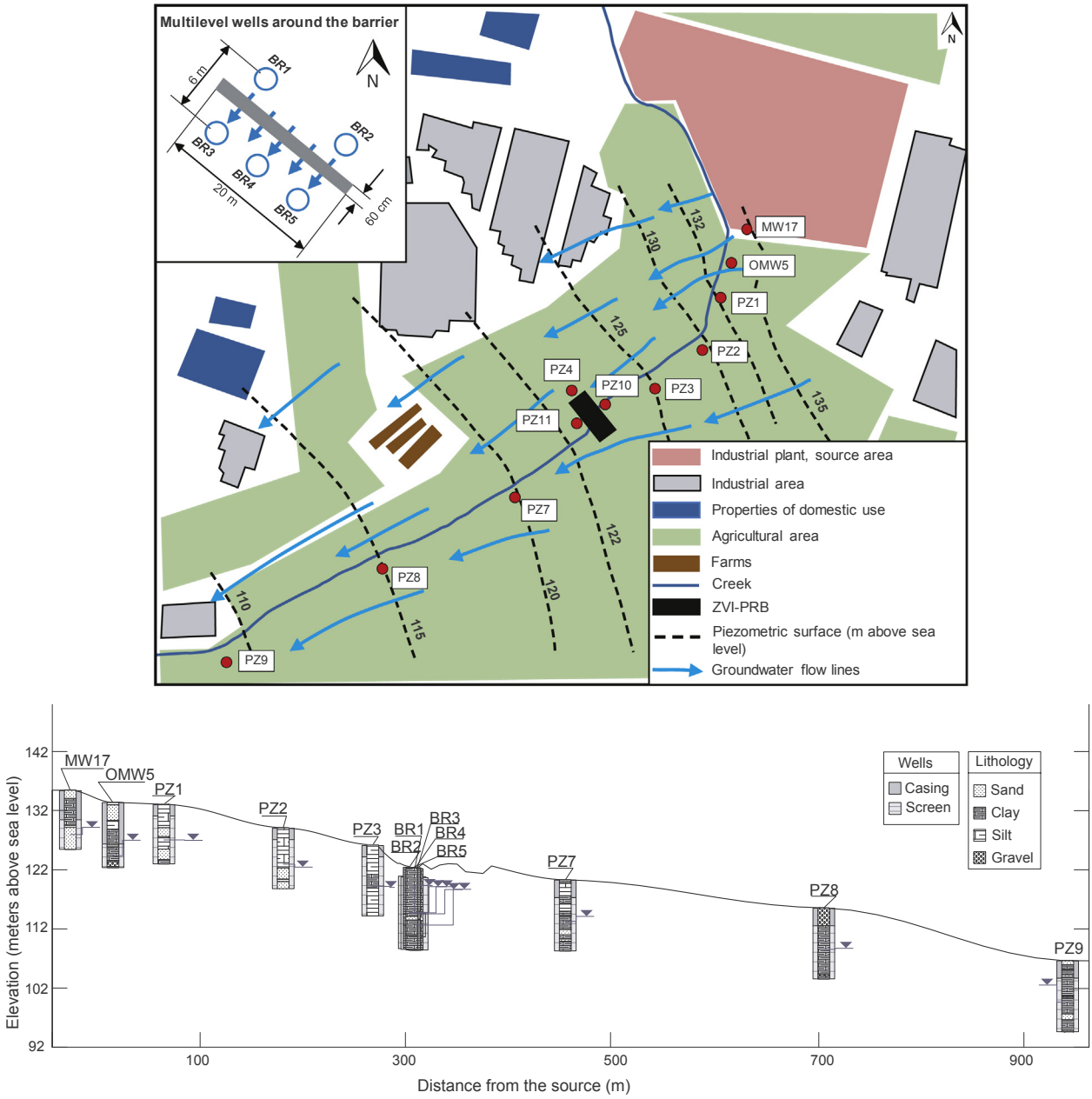

Fig. 1. Map of the study site. The location of the wells installed along Can Ninou Creek, the location of the ZVI-PRB, and the distribution of the multilevel wells around the ZVI-PRB, as well as the piezometric surfaces and groundwater flow lines, are represented. Cross section along the creek from the source area to 1000 m downstream. The lithology and the screened interval of each well is exposed, as well as the water table indicated by the blue triangles. Modified from Audí-Miró et al. (2015). (For interpretation of the references to colour in this figure legend, the reader is referred to the web version of this article.)

3. Materials and methods

3.1. Laboratory-scale experiments

Batch experiments were carried out in triplicate using 40 mL glass bottles. Each bottle contained 6.75 g of cast iron (92% purity, Gotthart Maier Metall pulver GmbH, Rheinfelden, Germany) and 35 mL of a nitrate-containing aqueous solution. Prior to the experiment, the ZVI was acid-cleaned with 1 N degassed HCl for 1 h and then rinsed five times with degassed deionized water (Milli-Q Plus UV, Millipore™, Billerica, Massachusetts, USA), dried and stored inside a sterilized and anaerobic chamber with a N_2 atmosphere at +28 ± 2 °C (Matheson and Tratnyek, 1994; Dayan et al., 1999; Slater et al., 2002). In the chamber, UV light was used to sterilize the iron. The ZVI was weighed before and after the treatment to verify that it was dry. The specific surface area of the cast iron determined by N_2 gas adsorption (BET method) (Brunauer et al., 1938) was 1.624 ± 0.007 $m^2\ g^{-1}$. The size of the iron particles ranged between 0.4 and 2.0 mm, with an average diameter of 1.2 mm (Torrentó et al., 2017).

Three different solutions were used: Milli-Q water (pH = 5.5) (MQ experiments), a pH 4 HCl 0.1 M solution (pH4 experiments) and groundwater (pH = 7.0) from a piezometer (PZ10) located immediately upgradient of the ZVI-PRB installed in the study site (PRB experiments). All of the synthetic solutions contained 1.93 mM of nitrate, whereas the content of nitrate in the groundwater sample was 2.93 mM.

The experiments were set up inside the glove box with an argon atmosphere to avoid the presence of O_2. After preparation, the bottles were immediately covered with aluminum foil to avoid oxidation due to light, and they were removed from the glove box and rotated on a horizontal roller table (Wheaton, Millville, New Jersey, USA) at 60 rpm

about their longitudinal axes. Experimental runs lasted for 8 days, and aqueous samples were taken daily using sterile syringes purged with N_2. All of the samples were filtered through a 0.2 µm Millipore® filter and preserved at 4 °C in darkness prior to further analysis. The concentrations of nitrogen species and the $\delta^{15}N$ and $\delta^{18}O$ of dissolved nitrate were measured in selected samples.

3.2. Sampling surveys

To assess the effect of the ZVI-PRB on the nitrate fate, three sampling campaigns were performed in June 2012, October 2012 and March 2013. Both the conventional and multilevel wells were sampled (Fig. 1). The conventional wells were sampled using a portable pump, whereas for the multilevel wells, disposable 60 mL polypropylene sterile syringes were used to raise the water from each small-diameter PTFE tube. In order to obtain depth discrete samples, the water volume sampled from each tube was minimized as much as possible to prevent interference with the adjacent tubes. For each sampling campaign, selected depths were sampled. For both conventional and multilevel wells, the wells were purged before sampling.

The groundwater piezometric level was measured and the physicochemical parameters (pH, temperature, dissolved oxygen and conductivity) were measured on site using a flow-through cell (Eijkelkamp, Netherlands) connected in line with the sampling tubes to avoid contact with the atmosphere. A Multi3410 multi-parameter meter (WTW, Weilheim, Germany) was used. Samples were collected and preserved in plastic bottles that were filled completely to avoid the oxidation of species from contact with the atmosphere. Samples were preserved at 4 °C and passed through a 0.2 µm filter in darkness prior to further analysis. In most of the collected samples, the nitrate, nitrite (NO_2^-), ammonium (NH_4^+) and cation concentrations were measured. The $\delta^{15}N$ and $\delta^{18}O$ of dissolved nitrate were measured in selected samples collected in March 2013. The δ^2H_{H2O} and $\delta^{18}O_{H2O}$ were analyzed in a subset of samples.

3.3. Analytical methods

Nitrate and nitrite concentrations were determined by high performance liquid chromatography (HPLC) with a WATERS 515 HPLC pump, IC-PAC anion columns and a WATERS 432 detector. Ammonium was analyzed using ionic chromatography (DIONEX ICS5000). For the analysis of major cations, samples were acidified with 1% nitric acid. The cation concentrations were determined by inductively coupled plasma-optical emission spectrometry (ICP-OES, Perkin-Elmer Optima 3200 RL). Chemical analyses were conducted at the "Centres Científics i Tecnològics" of the Universitat de Barcelona (CCiT-UB) and "Institut Català de Recerca de l'Aigua" (ICRA).

The $\delta^{15}N$ and $\delta^{18}O$ of dissolved nitrate were determined using a modified cadmium reduction method (McIlvin and Altabet, 2005; Ryabenko et al., 2009). Briefly, nitrate was converted to nitrite through spongy cadmium reduction and then to nitrous oxide using sodium azide in an acetic acid buffer. Simultaneous $\delta^{15}N$ and $\delta^{18}O$ analyses of the produced N_2O were carried out using a Pre-Con (Thermo Scientific) coupled to a Finnigan MAT-253 Isotope Ratio Mass Spectrometer (IRMS, Thermo Scientific). δ^2H_{H2O} was measured by pyrolysis using a Thermo-Quest high-temperature conversion analyzer (TC/EA) unit with a Finnigan MAT Delta C IRMS. $\delta^{18}O_{H2O}$ was measured using the CO_2 equilibrium technique following the standard method (Epstein and Mayeda, 1953) using a GasBench coupled to the MAT-253 IRMS. The notation was expressed in terms of δ relative to international standards (V-SMOW for δ^2H_{H2O} and $\delta^{18}O_{H2O}$ and V-AIR for $\delta^{15}N$). According to Coplen (2011), several international and laboratory standards were interspersed among the sequences for the normalization of analyses. The analytical reproducibility by repeated analysis of both international and internal reference samples of known isotopic composition was ± 1‰ for $\delta^{15}N_{NO3}$, ± 1.5‰ for $\delta^{18}O_{NO3}$, ± 1‰ for δ^2H_{H2O}, and ± 0.3‰ for $\delta^{18}O_{H2O}$. Samples for isotopic analyses were prepared at the MAiMA laboratory and determined at CCiT-UB.

3.4. Isotope fractionation calculation

Isotopic fractionation during nitrate transformation is commonly calculated in laboratory experiments in which the conditions are well constrained, no other sinks affect the nitrate pool and the changes in the concentration and the isotopic composition of nitrate can be considered to be exclusively determined by the nitrate transformation process. The process is modeled following a Rayleigh distillation. Using the Rayleigh equation (Eq. (4)), the isotopic fractionation factor α can be obtained (Aravena and Robertson, 1998; Mariotti et al., 1988):

$$ln\ (R_t/R_0) = (\alpha - 1) \times ln(C_t/C_0\ ) \quad (4)$$

where C_0 and C_t are the nitrate concentrations at the beginning and at a given time (t), respectively (mmol L^{-1}), and R_0 and R_t denote the ratios of heavy versus light isotopes at the beginning and at time t, respectively, which are calculated according to Eq. (5).

$$R = [(\delta/1000) + 1] \quad (5)$$

where δ is the isotopic composition of ^{15}N and ^{18}O (‰). The term $(\alpha - 1)$ is calculated from the slope of the regression analysis in double-logarithmic plots, $[\ln(R_t/R_0)]$ over $[\ln(C_t/C_0)]$, according to Eq. (4) and is converted to isotopic fractionation ($\varepsilon^{15}N$ and $\varepsilon^{18}O$) following Eq. (6).

$$\varepsilon = 1000 \times (\alpha - 1) \quad (6)$$

With the ε values obtained in the laboratory experiments, the percentage of denitrification at the field scale can be calculated according to Eq. (7) using either $\varepsilon^{15}N$ or $\varepsilon^{18}O$, or both.

$$DEN(\%) = \left[1 - \frac{[NO_3]_{residual}}{[NO_3]_{initial}}\right] \times 100 = \left[1 - e^{\left(\frac{\delta(residual) - \delta(initial)}{\varepsilon}\right)}\right] \times 100 \quad (7)$$

The isotope signature of the original nitrate ($\delta_{initial}$) is usually assumed to correspond to that of the determined nitrate source or to the lowest value found in the field site.

4. Results and discussion

4.1. Batch experiments: Chemical data

Complete removal of nitrate was observed within 7 days in all batch experiments (Supplementary Material, Table S1). In all experiments, ammonium was produced (maximum values of 2.47 mM for PRB, 1.47 mM for MQ and 1.40 mM for pH4), whereas no significant nitrite contents (maximum values for all experiments ranged from 0.01 mM to 0.03 mM, achieved during the first 2–3 days) were detected (Table S1). The nitrogen mass balance in the experiments shows that ammonium and nitrite account for approximately 50–100% of the nitrate removal in the PRB and 45–75% in the MQ and pH4 experiments (Table S1). According to Chen et al. (2005), sorption of ammonium onto mineral oxides produced by ZVI corrosion (Westerhoff and James, 2003) was ruled out. Thus, gaseous N species should account for closing the nitrogen mass balance. Production of N_2 (g) has been proposed to be a by-product of ZVI-driven nitrate reduction by other authors (Yang and Lee, 2005) in similar experiments. Furthermore, abiotic homogeneous or heterogeneous reduction of nitrite coupled to the oxidation of the Fe(II) released from the ZVI may also occur, which is also a source of N_2O (Buchwald et al., 2016).

Previous studies (Cheng et al., 1997; Choe et al., 2000; Su and Puls, 2004) have suggested that ZVI-driven nitrate reduction is first order with respect both nitrate concentration and ZVI concentration. Excluding the effect of ZVI concentration, the reaction was thus assumed to be of pseudo first order with respect to nitrate concentration. Data

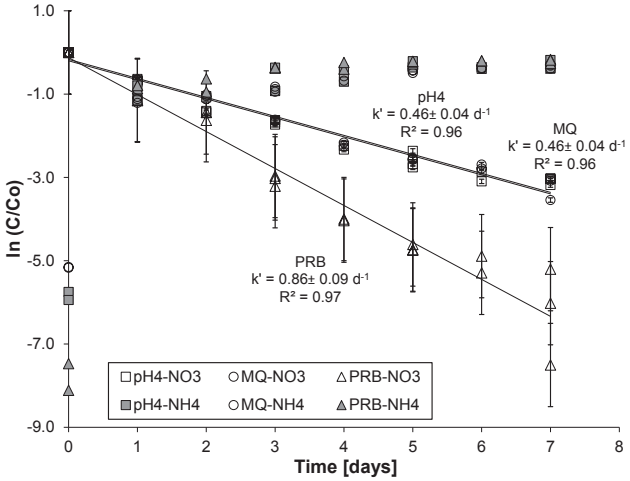

Fig. 2. Evolution of ln (C/C_0) for both nitrate and ammonium over time in all of the batch experiments. The linear regression lines and high correlation values (R^2) evidenced pseudo-first-order kinetics.

for nitrate concentration versus time were fit to a pseudo-first-order rate model:

$$\frac{dC}{dt} = -k' \times C \tag{8}$$

where C is the nitrate concentration, t is time and k' is the pseudo-first-order rate constant. The k' was obtained using the integrated form of this equation, from the slope of the regression lines of the ln C/C_0 vs. time graph (Fig. 2), where C_0 is the initial nitrate concentration. Uncertainty was obtained from the 95% confidence intervals. The nitrate consumption rate in the experiments with groundwater (PRB experiments) was faster (k' = 0.86 ± 0.09 d^{-1}) than that in the experiments with synthetic solutions (MQ and pH4 experiments, k' = 0.46 ± 0.04 d^{-1} for both experiments), suggesting additional nitrate degradation by autochthonous bacteria. The higher nitrate removal in biotic batch experiment (PRB) may be attributed to denitrification by autochthonous denitrifiers, which use the hydrogen or Fe (II) generated by ZVI corrosion as electron donors (Till et al., 1998; Shin and Cha, 2008; An et al., 2009; Jamieson et al., 2018; Xu et al., 2018; Zhang et al., 2019).

The surface-area-normalized reaction rate constants (k_{SA}) were calculated for comparison with other studies following Eq. (9) (Johnson et al., 1996):

$$dC/dt = -K'C = -K_{SA} \times a_s \times \rho_m \times C \tag{9}$$

where a_S is the ZVI specific surface area ($m^2\ g^{-1}$) and ρm is the mass concentration of ZVI ($g\ L^{-1}$).

The obtained k' values correspond to k_{SA} values of 2.8 ± 0.3 × 10^{-3} L m^{-2} d^{-1} for the PRB experiment and 1.6 ± 0.1 × 10^{-3} L m^{-2} d^{-1} for both the MQ and pH4 experiments. For the latter experiments, the obtained k_{SA} values are within the range reported for chemical nitrate reduction by ZVI (1.1 × 10^{-4} to 7.2 L m^{-2} d^{-1} for pH between 7 and 9.5, and 2.4 × 10^{-3} to 12.3 L m^{-2} d^{-1} for pH values of 3–6.5, Alowitz and Scherer, 2002; Su and Puls, 2004; Choe et al., 2004; Ginner et al., 2004; Miehr et al., 2004).

Both abiotic batch experiments (pH4 and MQ) showed the same reaction rate, suggesting that at the tested conditions (pH = 4 for the pH4 experiment, pH = 5.5 for the MQ experiment, respectively), ZVI-driven nitrate reduction was independent of the pH. Nevertheless, at pH values relevant to ZVI-PRBs (pH from 6.5 to 9), slower rates have generally been observed at higher pH values (Hu et al., 2001; Alowitz and Scherer, 2002; Miehr et al., 2004; Westerhoff and James, 2003; Ginner et al., 2004).

In the case of the experiment with combined abiotic nitrate reduction and denitrification (PRB experiment, since the ZVI surface area is not reported in most previous studies, a comparison is performed in terms of the pseudo-first-order rate constants. The k' value of the PRB experiment (k' = 0.86 ± 0.09 d^{-1}) is similar to that reported by Shin and Cha (2008) using a culture obtained from activated sludge and anaerobic digester samples from a wastewater treatment plant (k' = 0.97 d^{-1}), even when the latter used nano ZVI. Previous studies using cast (Ginner et al., 2004) and nano (An et al., 2009) ZVI in combination with pure cultures of denitrifying bacteria resulted in faster nitrate removal rates (k' from 1.5 to 2.4 d^{-1}).

4.2. Batch experiments: Isotopic results

All of the experiments showed considerable enrichment in both ^{15}N and ^{18}O in the remaining nitrate over the course of the experiments (Table S1), confirming nitrate degradation. In the PRB experiment, $\delta^{15}N$ increased from +8.2‰ to +154.9‰, whereas $\delta^{18}O$ increased from +5.4‰ to +83.5‰. Similarly, the $\delta^{15}N\text{-}NO_3^-$ in the MQ and pH4 experiments increased from +15.6‰ and +15.9‰ to +133.2‰ and +135.9‰, respectively. The $\delta^{18}O$ values increased from +26.5‰ and +29.3‰ to +78.2‰ and +79.9‰ in the MQ and pH4 experiments, respectively. The $\varepsilon^{15}N$ and $\varepsilon^{18}O$ values in the experiments were obtained from the slope of the linear correlation between the natural logarithm of the remaining fraction of the substrate, $\ln(C_{residual}/C_{initial})$, where C refers to the analyte concentration, and the determined isotope ratios, $\ln(R_{residual}/R_{initial})$, following Eq. (4) (Fig. 3). Uncertainty was obtained from the 95% confidence intervals. Obtained values are shown in Table 1. The nitrogen isotopic fractionation ($\varepsilon^{15}N$) was −29.5 ± 2.7‰ for the PRB experiment, −37.7 ± 7.2‰ for the MQ experiment and −36.1 ± 7.1‰ for pH4 experiment. The oxygen isotopic fractionation ($\varepsilon^{18}O$) was −16.4 ± 1.1‰ for the PRB experiment, −17.2 ± 4.2‰ for the MQ experiment, and −16.1 ± 3.1‰ for the pH4 experiment (Fig. 3).

The isotope fractionation for abiotic nitrate reduction has not been reported to date; the obtained values were thus compared with those reported for biotic denitrification. The $\varepsilon^{15}N$ and $\varepsilon^{18}O$ values obtained in the present study fell within the range of the values reported in the literature for denitrification in laboratory experiments (Grau-Martínez et al., 2017, and references therein). The $\varepsilon^{15}N$ values were similar to the values obtained by Barford et al. (1999) and Toyoda et al. (2005) for heterotrophic denitrification by pure cultures. With regards to $\varepsilon^{18}O$, the obtained values were similar to those reported by Wunderlich et al. (2012) for heterotrophic denitrification by pure cultures.

In all of the experiments, $\delta^{15}N$ showed a linear relationship with $\delta^{18}O$, with slopes between 0.43 and 0.54, yielding $\varepsilon^{18}O/\varepsilon^{15}N$ ratios of 0.54 ± 0.07 for the PRB experiment and 0.45 ± 0.02 and 0.43 ± 0.03 for the MQ and pH4 experiments, respectively (Fig. 4 and Table 1). A comparison of the obtained slopes for the regression lines ($\varepsilon^{18}O/\varepsilon^{15}N$) was performed by analysis of covariance (ANCOVA). Statistical significance was accepted at the $p < 0.05$ level. Since they were highly consistent, the data from the pH4 and MQ experiments were combined (Table 1). There is a significant statistical difference between the slope obtained for the experiments with purely abiotic solutions ($\varepsilon^{18}O/\varepsilon^{15}N$ = 0.43 ± 0.02) and that for the PRB experiment ($\varepsilon^{18}O/\varepsilon^{15}N$ = 0.54 ± 0.07) (ANCOVA, p = 0.0003). This result leads to the potential application of this approach to distinguish ZVI-driven nitrate reduction and additional degradation of nitrate by the action of autochthonous denitrifying bacteria in field sites where ZVI-PRBs are installed.

4.2.1. Insights from the $\varepsilon^{18}O/\varepsilon^{15}N$ ratio during abiotic ZVI-driven nitrate reduction

Abiotic nitrate reduction is the only process that acts in the MQ and pH4 batches. To the authors' knowledge, no isotopic fractionation ratio ($\varepsilon^{18}O/\varepsilon^{15}N$) for abiotic nitrate reduction using ZVI has been published to date. The $\varepsilon^{18}O/\varepsilon^{15}N$ reported for heterogeneous and homogeneous

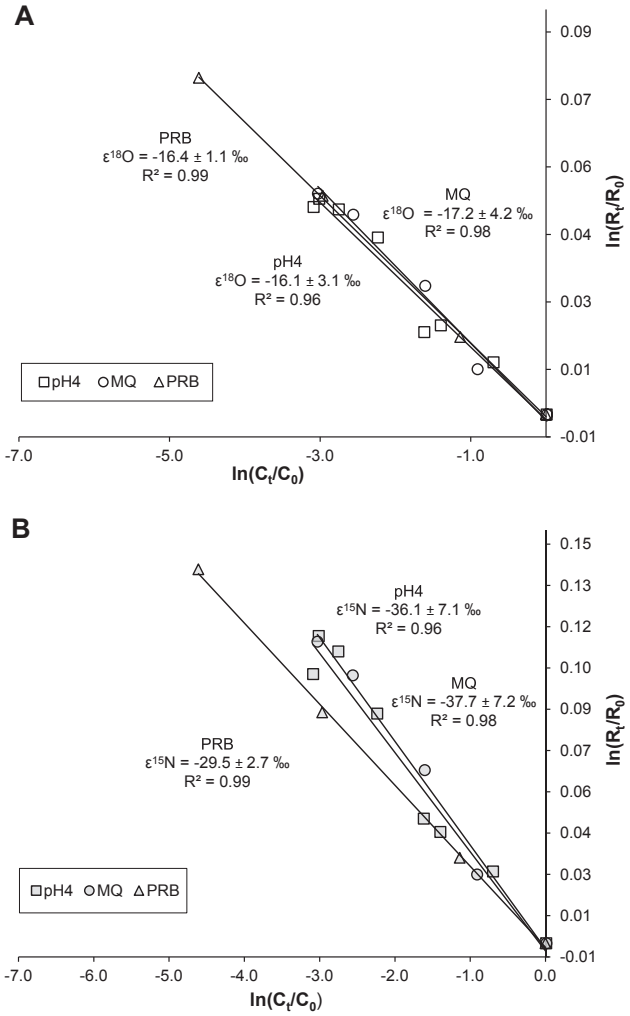

Fig. 3. $\delta^{18}O$ (A) and $\delta^{15}N$ (B) of nitrate against the natural logarithm of the nitrate concentration in the batch experiments. The slopes of the regression lines represent $(\alpha-1)$, the isotopic fractionation for N and O.

Table 1
Obtained N and O isotope fractionation values ($\varepsilon^{15}N$ and $\varepsilon^{18}O$) and isotope ratios ($\varepsilon^{18}O/\varepsilon^{15}N$) for the laboratory experiments.

	$\varepsilon^{15}N$ ± 95% CI	$\varepsilon^{18}O$ ± 95% CI	$\varepsilon^{18}O/\varepsilon^{15}N$ ± 95% CI
pH4	−36.1 ± 7.1	−16.1 ± 3.1	0.43 ± 0.05
MQ	−37.7 ± 7.2	−17.2 ± 4.2	0.45 ± 0.02
Combined pH4 & MQ	−36.6 ± 4.2	−16.4 ± 1.9	0.43 ± 0.02
PRB	−29.5 ± 2.7	−16.4 ± 1.0	0.54 ± 0.07
Denitrification in the PRB experiment*	−20.5	−15.5	0.76

* Estimated using Eq. (9), assuming that in the PRB experiment two competing pathways occurred: ZVI-driven nitrate reduction (i.e. combined pH4 & MQ) and denitrification. See the text for detailed information.

chemical nitrite reduction in the presence of dissolved Fe^{2+} showed higher values ($\varepsilon^{18}O/\varepsilon^{15}N$ from 0.7 to 1.7, Buchwald et al., 2016; Grabb et al., 2017). Lower ratios can be produced by the incorporation of oxygen isotopes from water into nitrite and the subsequent re-oxidation of nitrite to nitrate (Wunderlich et al., 2013). Consequently, the isotopic equilibrium tends to reduce the $\varepsilon^{18}O$ values, decreasing the $\varepsilon^{18}O/\varepsilon^{15}N$ ratio to values of 0.5. In this study, nitrite re-oxidation can be ruled out for all of the experiments since the batch experiments were performed under anaerobic conditions and nitrite accumulation was

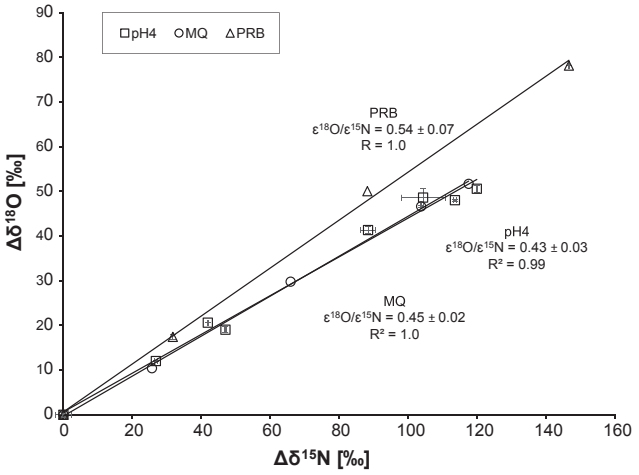

Fig. 4. $\Delta\delta^{15}N$ vs. $\Delta\delta^{18}O$ of nitrate for the batch experiments. The error bars show the uncertainty in the isotope measurements.

below 0.02 mM. Furthermore, in the pH4 and MQ experiments, with no biotic competition, the dissolved Fe^{2+} released from ZVI favored fast chemical nitrite reduction over any potential nitrate re-oxidation. In addition, the fast nitrate consumption and the high isotopic composition of $\delta^{18}O_{NO3}$ observed (up to +83.5‰) allowed us to consider the equilibrium isotopic fractionation between water and nitrate to be negligible compared with the kinetic isotopic fractionation during nitrate reduction. Lower $\varepsilon^{18}O/\varepsilon^{15}N$ ratios have also been reported to be produced by different enzymes involved in nitrate reduction (Granger et al., 2008). In this sense, the activity of the periplasmic nitrate reductase (Nap) results in a $\varepsilon^{18}O/\varepsilon^{15}N$ value of ~0.6, whereas the membrane-bound respiratory nitrate reductase (Nar) tends to produce a fractionation ratio of ~1.0 (Granger et al., 2008). The transformation of nitrate to ammonium by dissimilatory nitrate reduction to ammonium (DNRA) is considered to mostly be catalyzed by this Nap complex (Kraft et al., 2011). Therefore, the results of the MQ and pH4 experiments, without enzymatic function, suggest some mechanistic control in the isotope fractionation ratios obtained for purely chemical nitrate reduction by ZVI. On the other hand, although further research is needed, these results suggest that the use of $\varepsilon^{18}O/\varepsilon^{15}N$ to distinguish between biotic (DNRA) and abiotic (ZVI-driven) production of ammonium from nitrate reduction is limited.

4.2.2. Insights from the $\varepsilon^{18}O/\varepsilon^{15}N$ ratio during combined abiotic ZVI-driven nitrate reduction and denitrification

In the PRB experiment, a biotic nitrate-reduction process was assumed to occur in combination with a purely abiotic ZVI-driven nitrate reduction. This biotic nitrate reduction is likely to be autotrophic denitrification by autochthonous denitrifying bacteria using the hydrogen or the Fe^{2+} released from ZVI, although heterotrophic denitrification with the organic carbon present in groundwater or with the biogenic acetate produced by homoacetogens that utilize cathodic hydrogen cannot be ruled out (Zhang et al., 2019). From the kinetic data collected from all of the experiments (Fig. 2), the proportion of the ZVI-driven nitrate reduction (pathway 1) in the overall degradation process (pathway 1 + pathway 2) was calculated as the rate ratio of the two competing pathways ($F = k'_1/(k'_1 + k'_2)$), showing a 52% contribution of purely abiotic ZVI-driven nitrate reduction.

The isotopic fractionation values ($\varepsilon^{15}N$ and $\varepsilon^{18}O$) for the denitrification process in the PRB experiments (pathway 2) were then estimated using a Rayleigh-type equation for multiple competing degradation pathways following first-order kinetics (Van Breukelen, 2007), as follows (Eq. (10)):

$$F = \frac{\varepsilon_A - \varepsilon_2}{\varepsilon_1 - \varepsilon_2} \quad (10)$$

where ε_1 is the isotope fractionation of pathway 1 (ZVI-driven nitrate reduction, i.e., experiments pH4 and MQ), and ε_A is the isotope fractionation of the overall degradation process (i.e., the PRB experiment). The obtained values of $\varepsilon^{15}N$ (−15.5‰) and $\varepsilon^{18}O$ (−20.5‰) for the denitrification process in the PRB experiments were used to estimate the corresponding $\varepsilon^{18}O/\varepsilon^{15}N$ ratio ($\varepsilon^{18}O/\varepsilon^{15}N$ = 0.76) (Table 1).

During (heterotrophic and autotrophic) denitrification, the $\varepsilon^{18}O/\varepsilon^{15}N$ ratio reported in laboratory studies ranged from 0.3 (Knöller et al., 2011) to 1.3 (Grau-Martínez et al., 2018) in freshwater environments, whereas in marine environments, the fractionation ratio showed values of ~1.0 (Casciotti et al., 2002; Granger et al., 2004; Sigman et al., 2005). Autotrophic denitrification experiments using pyrite (FeS_2) as an electron donor have shown a fractionation ratio of 0.87 (Torrentó et al., 2010). A $\varepsilon^{18}O/\varepsilon^{15}N$ ratio of 0.9 has been reported for autotrophic denitrification with aqueous Fe^{2+} in groundwater (Smith et al., 2017). To the authors' knowledge, the isotopic fractionation ratio for hydrogenotrophic denitrification has not been reported and cannot be compared with the obtained results. Factors such as the pH, salinity or carbon sources showed no effect on the $\varepsilon^{18}O/\varepsilon^{15}N$ ratio (Granger et al., 2008; Wunderlich et al., 2012). Nevertheless, the microbial community composition can impact the ratio at which the nitrogen and oxygen of nitrate are processed during denitrification (Dähnke and Thamdrup, 2016). Overall, despite the fact that the differences between the $\varepsilon^{18}O/\varepsilon^{15}N$ ratios obtained for PRB and those of the pH4 and MQ experiments suggest the occurrence of denitrification in the former, the responsible reaction could not be addressed.

4.3. Field study

4.3.1. Hydrochemical characterization

The results of the chemical characterization of the field samples are detailed in the Supplementary Material (Table S2). The pH values analyzed upgradient of the barrier ranged between 6.7 and 9.0, whereas the pH values of the multilevel (BR1, BR2, BR3, BR4, BR5) and conventional (PZ10 and PZ11) wells located close to the barrier ranged between 4.4 and 7.5, except for higher values that were found in a few points in June 2012. The PZ4 well, located at the west end of the barrier, presented pH values of approximately 7 in June 2012 and approximately 9 in March 2013. Finally, the pH values in conventional wells downgradient of the ZVI-PRB ranged from 5.4 to 8.8, similar to the values observed upgradient of the PRB. The pH analyzed downgradient of the barrier therefore does not correspond to the common increase of pH that usually occurs after the corrosion of iron with water (Eq. (2)), probably due to the relatively high pH-buffering capacity of the aquifer.

The chemical data indicated that reducing conditions prevailed in the aquifer: dissolved oxygen (DO) was found in most of the points below 2 mg L^{-1}; dissolved manganese was present at a concentration up to 1.39 mg L^{-1}; and dissolved iron was detected at a concentration up to 2.5 mg L^{-1}. Furthermore, Audí-Miró et al. (2015) demonstrated that these conditions were conducive to the biodegradation of chlorinated ethenes by reductive dechlorination.

To assess the effect of ZVI-PRB on nitrogen compounds, the evolution of the nitrate, nitrite and ammonium concentrations was monitored along the flow path, upgradient and downgradient of the ZVI-PRB. The samples in the focus area (MW-17) showed negligible nitrate concentrations throughout the sampling period, indicating that reducing conditions prevailed. In this well, the presence of dissolved manganese and iron was up to 1.3 mg L^{-1} and 2.5 mg L^{-1}, respectively, confirming reducing conditions. Downgradient of the focus area, wells OMW5, PZ1, PZ2 and PZ3 showed low nitrate values (up to 29.4 mg L^{-1}, Table S2) in all campaigns.

Fig. 5 shows the evolution of the nitrate concentrations in the wells closer to the barrier (the conventional wells PZ10, PZ4 and PZ11 and the multilevel wells BR1, BR2, BR3, BR4 and BR5) for the three sampling surveys. Overall, there are no significant differences in the nitrate concentration with depth. The nitrate concentrations in these wells increase throughout the sampling period, with median concentrations of approximately 79 mg L^{-1} (June 2012), 141 mg L^{-1} (October 2012) and 177 mg L^{-1} (March 2013).

Regarding multilevel wells located immediately upgradient and downgradient of the PRB, the nitrate concentrations are always higher in piezometers BR1 and BR3, both of which are located to the NW of the barrier, and lower in piezometers BR2, BR4 and BR5, which are located to the SE of the PRB. These results are probably due to the lateral input of water with a high nitrate concentration (the conventional well PZ4, located to the NW of the barrier, has the highest nitrate concentration). Because of this observed lateral input, the percentage of nitrate attenuation due to the barrier was calculated from the nitrate contents by comparing BR1 to BR3 and BR2 to BR4 and BR5. Comparing BR1 to BR3, a slight decrease in the nitrate concentration was observed in June 2012 and October 2012 (16% decrease) and March 2013 (11% decrease). Comparing BR2 to BR4 and BR5, a higher decrease in the nitrate concentration was observed in June 2012 (26–72%) and October 2012 (30%), whereas in March 2013, contradictory percentages were obtained (an increase of 10% between BR2 and BR4 and an 18% decrease between BR2 and BR5). Therefore, the observed changes in the nitrate concentration from immediately upgradient to downgradient of the PRB suggest the occurrence of nitrate degradation processes related to the ZVI-PRB, although isotope data are required to confirm this hypothesis. No significant differences in nitrite concentrations were observed upgradient and downgradient of the barrier, since in most cases, they were below the detection limit (0.01 mg L^{-1}). The ammonium concentration slightly increased from BR2 to BR4 and BR5 in June 2012, but values were always below 0.4 mg L^{-1}. No significant ammonium was detected downgradient of the barrier, indicating that if nitrate was transformed to ammonium through a reaction with the ZVI, it was oxidized again to nitrate or absorbed into soil materials.

The wells located far downgradient of the ZVI-PRB (PZ7, PZ8 and PZ9) showed nitrate concentrations ranging from 14 mg L^{-1} to 80 mg L^{-1} (Table S2). For the three sampling campaigns, lower values were observed in PZ7 and increased downgradient. This downgradient increase could reflect the contribution of lateral inputs or the fact that the barrier was bypassed. In these points, no significant differences in nitrite and ammonium concentrations were observed.

4.3.2. Evidence of nitrate reduction: Insights from isotope data

The results of the isotopic characterization of the field samples are detailed in the Supplementary Material (Table S3). The samples from the focus zone (MW17) could not be analyzed because the nitrate concentrations were below the detection limit, which is in agreement with the observed reducing conditions and the natural biodegradation of chlorinated solvents described previously by Audí-Miró et al. (2015). Wells OMW5 and PZ2, located upgradient of the PRB, showed isotopic values of approximately +15‰ for $\delta^{15}N_{NO3}$ and +11‰ for $\delta^{18}O_{NO3}$. These high values suggest that natural attenuation of nitrate takes place upgradient of the ZVI-PRB. Audí-Miró et al. (2015) also observed the natural attenuation for chlorinated solvents in these wells.

Fig. 6 shows the $\delta^{15}N_{NO3}$ and $\delta^{18}O_{NO3}$ from the survey of March 2013 at the multilevel wells (BR 1–5) and the conventional wells located closer to the PRB (PZ4 and PZ10). The isotopic values of the main potential nitrate sources are represented as well: nitrate fertilizers, ammonium fertilizers, soil nitrate and animal manure or sewage (Vitòria et al., 2004; Kendall et al., 2007; Xue et al., 2009). The range of $\delta^{18}O$ of nitrate derived from nitrification of ammonium fertilizers, soil nitrogen and/or manure/sewage (from +1.9‰ to +3.1‰) was estimated according to Anderson and Hooper (1983) using the range of $\delta^{18}O_{H2O}$ measured in groundwater samples (between −7.6‰ and −5.1‰). All of the samples presented isotope ratios compatible with

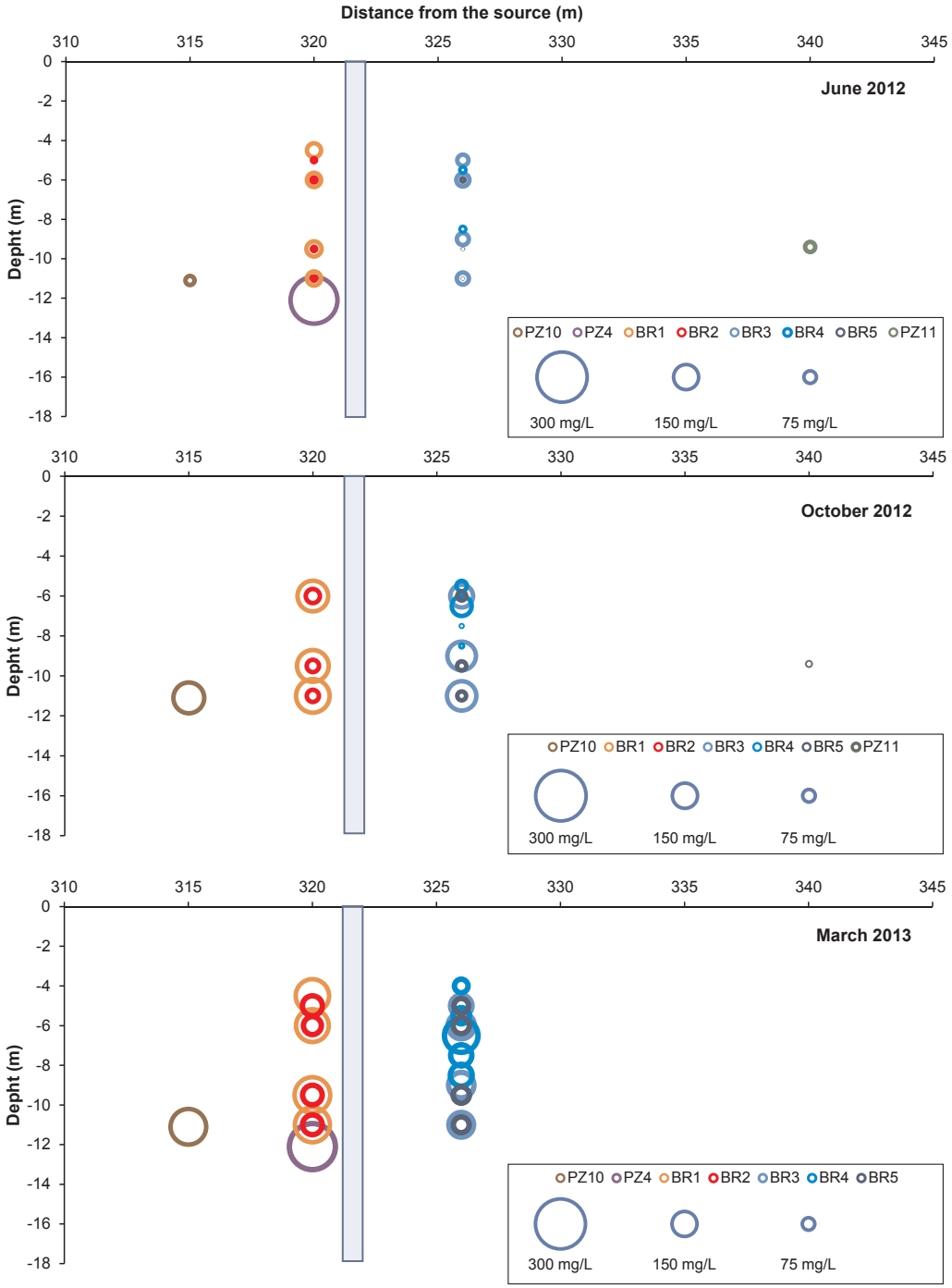

Fig. 5. Nitrate concentrations by depth in the surroundings of the PRB. The different depths of the multilevel wells are shown, as well as those of two conventional wells located immediately upgradient (PZ10) and downgradient (PZ11) of the PRB (blue rectangle). The well PZ4, located in the NW end of the PRB, is also shown. The size of the symbols is proportional to the corresponding nitrate concentration value. Reference concentration values are shown for comparison. (For interpretation of the references to colour in this figure legend, the reader is referred to the web version of this article.)

those for soil organic nitrogen and manure/sewage, with variable degree of denitrification. The nitrogen and oxygen isotope values of the samples located immediately upgradient of the PRB ranged from +6.2 to +13.9‰ for $\delta^{15}N$ and from +4.9 to +9.7‰ for $\delta^{18}O$, whereas the values of the samples located immediately downgradient of the PRB ranged from +13.2 to +18.1‰ for $\delta^{15}N$ and from +9.0 to +12.6‰ for $\delta^{18}O$, except for BR5-11, where low isotope ratios were obtained (+9.6‰ and +6.8‰, respectively). Taking into account that the PRB is located at a depth of approximately 10 m, a bypass effect probably occurs at the BR5-11 point, where low isotope ratios were obtained. It is important to note that PZ4 and BR1 showed higher values of $\delta^{15}N_{NO3}$ and $\delta^{18}O_{NO3}$ than those for BR2, which confirms that both PZ4 and BR1 are affected by a lateral input of groundwater with higher nitrate concentration and different isotope signature. Therefore, in general, higher isotopic values were detected immediately downgradient than immediately upgradient of the PRB, confirming the existence of nitrate attenuation processes. Furthermore, the samples showed a positive correlation ($r^2 = 0.89$) between $\delta^{15}N_{NO3}$ and $\delta^{18}O_{NO3}$ and were aligned following a $\varepsilon^{18}O/\varepsilon^{15}N$ ratio of 0.63 (Fig. 6), which is consistent with denitrification (Kendall et al., 2007) and with the values obtained in the

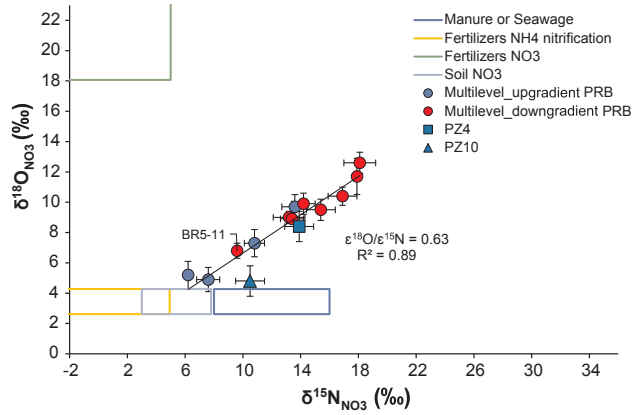

Fig. 6. $\delta^{15}N_{NO3}$ and $\delta^{18}O_{NO3}$ in groundwater samples collected in March 2013 for the multilevel wells and two conventional wells located immediately upgradient of the PRB (PZ4 and PZ10), as well as the isotope composition of the main potential nitrate sources: fertilizers, soil nitrate and animal manure or sewage.

PRB experiments.

We thus assumed the occurrence of combined ZVI-driven nitrate reduction and denitrification. To quantify the efficiency of the ZVI-PRB in removing nitrate, Eq. (7) was applied using the $\varepsilon^{15}N$ and $\varepsilon^{18}O$ values calculated in the PRB batch experiments ($\varepsilon^{15}N = -29.5 \pm 2.7$‰ and $\varepsilon^{18}O = -16.4 \pm 1.1$‰). Since some wells were affected with the lateral input of groundwater contaminated with nitrate with a different isotope signature, two $\delta_{initial}$ values were used: (1) the initial isotopic composition of the PRB experiment (+8.2‰ for $\delta^{15}N_{NO3}$ and +5.4‰ for $\delta^{18}O_{NO3}$), which corresponds to water extracted from PZ10, located upgradient of the barrier but not affected by the lateral input of PZ4 (model % DEN), and (2) the average isotope ratios of the PZ4 and BR1 wells (+12.8‰ for $\delta^{15}N_{NO3}$ and + 8.5‰ for $\delta^{18}O_{NO3}$), which are clearly affected by the lateral input of PZ4 (model % DEN Lateral). Fig. 7 shows the ranges of percentage of nitrate degradation obtained applying the two models and the isotope signature of the multilevel wells and the PZ4 and PZ10 wells. The %DEN Lateral model was thus used for the well BR3, which was clearly affected by the lateral input. The degree of nitrate attenuation in the samples of this well ranged between 10 and 20%. Similar though slightly lower percentages (5–15%) were obtained for samples of the BR5 well, for which the % DEN model was used. Finally, the results from samples from BR4 suggest that this well might also be affected by the lateral input of PZ4, and

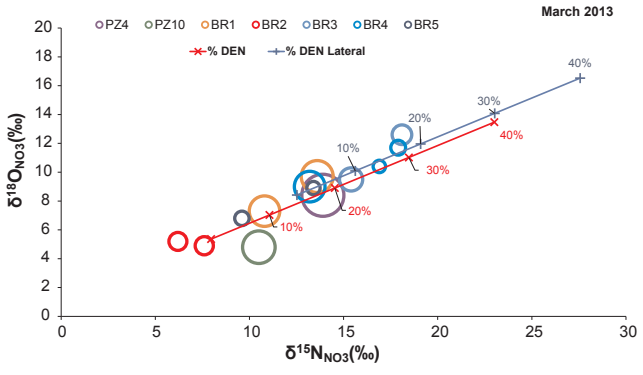

Fig. 7. $\delta^{15}N_{NO3}$ vs. $\delta^{18}O_{NO3}$ in groundwater samples collected in March 2013 for the multilevel wells and for two conventional wells located immediately upgradient of the PRB (PZ4 and PZ10). The size of the bubbles is proportional to the nitrate concentration. The denitrification models calculated with the Rayleigh equation using the isotopic fractionation obtained in the PRB experiment and two different initial values, one affected by the lateral input of PZ4 (% DEN Lateral) and one not affected (% DEN), are also shown.

thus the %DEN Lateral model was used, obtaining a degree of degradation of approximately 15%.

Overall, the nitrate removal percentages calculated using the isotopic model are in agreement with those calculated using the nitrate concentration. On well BR5, this percentage was slightly overestimated using only chemical data, because bypass could only be detected using isotopic data. The isotopic data also allowed the identification of the influence of the lateral input of PZ4 not only on BR3 but also on BR4. Therefore, stable isotopes of dissolved nitrate are powerful tools to assess the efficacy of the barrier for nitrate removal.

For further quantitative evaluation of the effect of the ZVI-PRB on the nitrate fate, by means of the data obtained in the laboratory experiments, the contribution of the purely abiotic ZVI-driven reaction in overall nitrate consumption was calculated using the equation proposed by Van Breukelen (2007) for estimating the distribution (F) of two competing pathways based on the two-dimensional isotopes approach (Eq. (11)):

$$F = \frac{(\varepsilon O_A/\varepsilon N_A \times \varepsilon N_2) - \varepsilon O_2}{(\varepsilon O_1 - \varepsilon O_2) - [\varepsilon O_A/\varepsilon N_A \times (\varepsilon N_1 - \varepsilon N_2)]} \quad (11)$$

where $\varepsilon^{18}O_A/\varepsilon^{15}N_A$ corresponds to the ratio of 0.63 obtained for the wells located immediately upgradient and downgradient of the PRB (Fig. 6). The $\varepsilon^{18}O$ and $\varepsilon^{15}N$ values obtained in the laboratory experiments were used for pathway 1 (purely abiotic ZVI-PRB driven nitrate reduction, i.e., MQ experiment, Table 1) and pathway 2 (denitrification, i.e., values obtained by Eq. (10), Table 1). The results show that approximately 30% of the nitrate consumption was related to the purely abiotic nitrate reduction by the ZVI included in the PRB.

Overall, the isotopic results confirm that nitrate reduction is taking place in the barrier, though it has a limited effect (maximum attenuation degree of 15–20%). This result is in agreement with the previous results of Audí-Miró et al. (2015), in which the effectiveness of the ZVI-PRB to reduce chlorinated solvents was tested using isotopic tools and was demonstrated to be even less efficient than for nitrate (maximum of 10%). The O-N slope of field values fit the expected slope obtained in the laboratory experiments well, indicating that isotopes are an excellent tool to determine the efficacy of the ZVI-PRB at the field scale.

5. Conclusions

In laboratory experiments with sterilized ZVI and synthetic nitrate solutions, ZVI induced nitrate reduction, mainly releasing ammonium to solution (after 7 days, ammonium accounted for 70–80% of nitrate reduction). For assessing the fate of nitrate in the contaminated site of Granollers, where a ZVI-PRB was installed, batch experiments were also performed using ZVI and groundwater from the study area. In these experiments, the main final product was also ammonium (80–100%). The faster nitrate removal rates of the latter suggest denitrification processes in addition to the ZVI-driven purely abiotic nitrate reduction. Isotopic fractionation associated to ZVI-induced nitrate attenuation processes was determined for the first time. The significant statistical difference between the isotope $\varepsilon^{18}O/\varepsilon^{15}N$ ratios obtained for the experiments with purely abiotic solutions (0.43 ± 0.02) and for the PRB experiment (0.54 ± 0.07) shows the potential for the use of this approach to distinguish ZVI-driven nitrate reduction and additional degradation of nitrate by the action of autochthonous bacteria in field sites where ZVI-PRBs are installed. Data obtained from the laboratory experiments were used for assessing the fate of nitrate in the study area. Combining chemical and isotope data, it was demonstrated that the ZVI-PRB installed in the study area locally induced nitrate attenuation, though the barrier had a limited effect (less than 15–20%). As Audí-Miró et al. (2015) noted for chlorinated solvents, this low efficiency in nitrate removal was probably related to the non-optimal design of the PRB, including a ZVI amount (3%) that was too low and an insufficient length of the PRB, which was responsible for the bypass occurrence. Further evaluation of the fate of ammonium downgradient of the ZVI-

PRB is required since no ammonium was detected in groundwater. Laboratory experiments can be performed to assess the potential retention of the generated ammonium by the aquifer materials through ion exchange and/or adsorption. Further work is required to identify the reaction responsible for the additional nitrate removal in experiments with ZVI and groundwater from the field site and to study the denitrifying microbial community developed around the ZVI-PRB. Overall, this study highlights the potential of isotope tools for determining the efficacy of nitrate removal by ZVI-PRBs at the field scale. This information might be crucial for mitigating existing pollution in water resources and improving remediation actions.

Conflict of interest

None.

Acknowledgments

This work has been financed by the projects: REMEDIATION (CGL2014-57215-C4) and PACE-ISOTEC (CGL2017-87216-C4-1-R), both financed by the Spanish Government and the AEI/FEDER from the EU, and MAG (2017 SGR 1733), from the Catalan Government. We would like to thank the CCiT of the Universitat de Barcelona for the analytical support. We thank the editor and four anonymous reviewers for comments that improved the quality of the manuscript.

Appendix A. Supplementary data

Supplementary data to this article can be found online at https://doi.org/10.1016/j.jhydrol.2018.12.049.

References

Alowitz, M.J., Scherer, M.M., 2002. Kinetics of nitrate, nitrite, and Cr(VI) reduction by iron metal. Environm. Sci. Technol. 36, 299–306.
An, Y., Li, T.L., Jin, Z.H., Dong, M.Y., Li, Q.Q., 2009. Decreasing ammonium generation using hydrogenotrophic bacteria in the process of nitrate reduction by nanoscale zero-valent iron. Sci. Total Environ. 407, 5465–5470.
Anderson, K.K., Hooper, A.B., 1983. O_2 and H_2O are each the source of O in NO_2 produced from NH_3 by Nitrosomas: ^{1}5N-NMR evidence. FEBS Lett. 64, 236–240.
Aravena, R., Robertson, W.D., 1998. Use of multiple isotope tracers to evaluate denitrification in ground water: study of nitrate from a large-flux septic system plume. Ground Water 36, 975–982.
Audí-Miró, C., Cretnik, S., Torrentó, C., Rosell, M., Shouakar-Stash, O., Otero, N., Palau, J., Elsner, M., Soler, A., 2015. C, Cl and H compound specific isotope analysis to assess natural versus Fe(0) barrier-induced degradation of chlorinated ethenes at a contaminated site. J. Hazar. Mater. 299, 747–754.
Barford, C.C., Montoya, J.P., Altabet, M.A., Mitchell, R., 1999. Steady-state nitrogen isotope effects of N_2 and N_2O production in *Paracoccus denitrificans*. Appl. Environm. Microbiol. 65, 989–994.
Brunauer, S., Emmet, P.H., Teller, E., 1938. Adsorption of gases on multimolecular layers. J. Am. Chem. Soc. 60, 309–319.
Buchwald, C., Grabb, K., Hansel, C.M., Wankel, S.D., 2016. Constraining the role of iron in environmental nitrogen transformations: dual stable isotope systematics of abiotic NO_2^- reduction by Fe(II) and its production of N_2O. Geochim. Cosmochim. Ac. 186, 1–12.
Casciotti, K.L., Sigman, D.M., Hastings, M.G., Böhlke, J.K., Hilkert, A., 2002. Measurement of the oxygen isotopic composition of nitrate in seawater and freshwater using the denitrifier method. Anal. Chem. 74, 4905–4912.
Chen, Y.M., Li, C.W., Chen, S.S., 2005. Fluidized zero valent iron bed reactor for nitrate removal. Chemosphere 59, 753–759.
Cheng, I.F., Muftikian, R., Fernando, Q., Korten, N., 1997. Reduction of nitrate to ammonia by zero-valent iron. Chemosphere 35, 2689–2695.
Choe, S., Chang, Y.Y., Hwang, K.Y., Khim, J., 2000. Kinetics of reductive denitrification by nanoscale zero-valent iron. Chemosphere 41, 1307–1311.
Choe, S., Liljestrand, H.M., Khim, J., 2004. Nitrate reduction by zero-valent iron under different pH regimes. Appl. Geochem. 19, 335–342.
Coplen, T.B., 2011. Guidelines and recommended terms for expression of stable-isotope-ratio and gas-ratio measurement results. Rapid Commun. Mass Sp. 25, 2538–2560.
Dähnke, K., Thamdrup, B., 2016. Isotope fractionation and isotope decoupling during anammox and denitrification in marine sediments. Limnol. Oceanogr. 61, 610–624.
Daniels, L., Belay, N., Rajagopal, P., Weimer, J., 1987. Bacterial methanogenesis and the growth of CO_2 with elemental iron as the sole source of electrons. Science 237, 509–511.
Da Silva, M.L.B., Johnson, R.L., Alvarez, P.J.J., 2007. Microbial characterization of groundwater undergoing treatment with a permeable reactive iron barrier. Environ. Eng. Sci. 24, 1122–1127.
Dayan, H., Abrajano, T., Sturchio, N.C., Winsor, L., 1999. Carbon isotopic fractionation during reductive dehalogenation of chlorinated ethenes by metallic iron. Org. Geochem. 30, 755–763.
Della Rocca, C., Belgiorno, V., Meric, S., 2006. An heterotrophic/autotrophic denitrification (HAD) approach for nitrate removal from drinking water. Process. Biochem. 41, 1022–1028.
Della Rocca, C., Belgiorno, V., Meric, S., 2007. Overview of in-situ applicable nitrate removal processes. Desalination 204, 46–62.
Dejournett, T.D., Alvarez, P.J., 2000. Combined microbial-Fe (0) treatment system to remove nitrate from contaminated groundwater. Biorem. J. 4, 149–154.
Epstein, S., Mayeda, T., 1953. Variation of O^{18} content of waters from natural sources. Geochim. Cosmochim. Ac. 4, 213–224.
Flury, B., Eggenberger, U., Mäder, U., 2009. First results of operating and monitoring an innovative design of a permeable reactive barrier for the remediation of chromate contaminated groundwater. Appl. Geochem. 24, 687–696.
Ginner, J.L., Alvarez, P.J., Smith, S.L., Scherer, M.M., 2004. Nitrate and nitrite reduction by Fe0: influence of mass transport, temperature, and denitrifying microbes. Environm. Eng. Sci. 21, 219–229.
Grabb, K.C., Buchwald, C., Hansel, C.M., Wankel, S.D., 2017. A dual nitrite isotopic investigation of chemodenitrification by mineral-associated Fe (II) and its production of nitrous oxide. Geochim. Cosmochim. Ac. 196, 388–402.
Granger, J., Sigman, D.M., Needoba, J.A., Harrison, P.J., 2004. Coupled nitrogen and oxygen isotope fractionation of nitrate during assimilation by cultures of marine phytoplankton. Limnol. Oceanogr. 49, 1763–1773.
Granger, J., Sigman, D.M., Lehmann, M.F., Tortell, P.D., 2008. Nitrogen and oxygen isotope fractionation during dissimilatory nitrate reduction by denitrifying bacteria. Limnol. Oceanogr. 53, 2533–2545.
Grau-Martínez, A., Torrentó, C., Carrey, R., Rodríguez-Escales, P., Domènech, C., Ghiglieri, G., Soler, A., Otero, N., 2017. Feasibility of two low-cost organic substrates for inducing denitrification in artificial recharge ponds: batch and flow-through experiments. J. Contam. Hydrol. 198, 48–58.
Grau-Martínez, A., Folch, A., Torrentó, C., Valhondo, C., Barba, C., Domènech, C., Soler, A., Otero, N., 2018. Monitoring induced denitrification during managed aquifer recharge in an infiltration pond. J. Hydrol. 561, 123–135.
Gu, B., Watson, D.B., Phillips, D.H., Liang, L., 2002a. Biogeochemical, mineralogical, and hydrological characteristics of an iron reactive barrier used for treatment of uranium and nitrate. In: Naftz, D.L., Morrison, S.J., Davis, J.A., Fuller, C.C. (Eds.), Groundwater remediation of trace metals, radionuclides, and nutrients with Permeable Reactive Barriers. Academic Press, New York, pp. 305–342.
Gu, B., Watson, D.B., Wu, L., Phillips, D.H., White, C., Zhou, J.Z., 2002b. Microbiological characteristics in a zero-valent iron reactive barrier. Environ. Monit. Assess. 77, 293–309.
Hosseini, S.M., Tosco, T., 2015. Integrating NZVI and carbon substrates in a non-pumping reactive wells array for the remediation of a nitrate contaminated aquifer. J. Contam. Hydrol. 179, 182–195.
Hosseini, S.M., Tosco, T., Ataie-Ashtiani, B., Simmons, C.T., 2018. Non-pumping reactive wells filled with mixing nano and micro zero-valent iron for nitrate removal from groundwater: vertical, horizontal, and slanted wells. J. Contam. Hydrol. 210, 50–64.
Hu, H.-Y., Naohiro, G., Koichi, F., 2001. Effect of pH on the reduction of nitrite in water by metallic iron. Water Res. 35, 2789–2793.
Huang, Y.H., Zhang, T.C., 2004. Effects of low pH on nitrate reduction by iron powder. Water Res. 38, 2631–2642.
Huang, C.P., Wang, H.W., Chiu, P.C., 1998. Nitrate reduction by iron at near neutral pH. J. Environ. Engineer. ASCE 128, 604–611.
Huang, G., Huang, Y., Hu, H., Liu, F., Zhang, Y., Deng, R., 2015. Remediation of nitrate-nitrogen contaminated groundwater using a pilot-scale two-layer heterotrophic-autotrophic denitrification permeable reactive barrier with spongy iron/pine bark. Chemosphere 130, 8–16.
Hwang, Y.H., Kim, D., Shin, H., 2011. Mechanism study of nitrate reduction by nano zero valent iron. J. Hazard. Mater. 185, 1513–1521.
Jamieson, J., Prommer, H., Kaksonen, A.H., Sun, J., Siade, A.J., Yusov, A., Bostick, B., 2018. Identifying and quantifying the intermediate processes during nitrate-dependent iron (II) oxidation. Environm. Sci. Technol. 52, 5771–5781.
Johnson, T.L., Scherer, M.M., Tratnyek, P.G., 1996. Kinetics of halogenated organic compound reduction by iron metal. Environ. Sci. Technol. 30, 2634–2640.
Johnson, R., Tratnyek, P., 2008. Remediation of Explosives in Groundwater Using a Zero-Valent Iron Permeable Reactive Barrier. ESTCP Project ER-0223. Science University, Portland.
Kamolpornwijit, W., Liang, L., West, O.R., Moline, G.R., Sullivan, A.B., 2003. Preferential flow path development and its influence on long-term PRB performance: column study. J. Contam. Hydrol. 66, 161–178.
Kendall, C., Elliott, E.M., Wankel, S.D., 2007. Tracing anthropogenic inputs of nitrogen to ecosystems. In: Michener, R.H., Lajtha, K. (Eds.), Stable Isotopes in Ecology and Environmental Science. Blackwell Publishing, pp. 375–449.
Khan, F.I., Husain, T., Hejazi, R., 2004. An overview and analysis of site remediation technologies. J. Envirn. Manage. 71, 95–122.
Knöller, K., Vogt, C., Haupt, M., Feisthauer, S., Richnow, H.H., 2011. Experimental investigation of nitrogen and oxygen isotope fractionation in nitrate and nitrite during denitrification. Biogeochemistry 103, 371–384.
Kraft, B., Strous, M., Tegetmeyer, H.E., 2011. Microbial nitrate respiration – genes, enzymes and environmental distribution. J. Biotechnol. 155, 104–117.
Liang, L., Moline, G.R., Kamolpornwijit, W., West, O.R., 2005. Influence of hydrogeochemical processes on zero-valent iron reactive barrier performance: a field investigation. J. Contam. Hydrol. 78, 291–312.

Liu, Y.S., Ying, G.G., Shareef, A., Kookana, R.S., 2013. Biodegradation of three selected benzotriazoles in aquifer materials under aerobic and anaerobic conditions. J. Contam. Hydrol. 151, 131–139.
Mariotti, A., Landreau, A., Simon, B., 1988. ^{15}N isotope biogeochemistry and natural denitrification process in groundwater application to the chalk aquifer of northern France. Geochim. Cosmochim. Ac. 52, 1869–1878.
Matheson, L.J., Tratnyek, P.G., 1994. Reductive dehalogenation of chlorinated methanes by iron metal. Environ. Sci. Technol. 28, 2045–2053.
McIlvin, M.R., Altabet, M.A., 2005. Chemical conversion of nitrate and nitrite to nitrous oxide for nitrogen and oxygen isotopic analysis in freshwater and seawater. Anal. Chem. 77, 5589–5595.
Miehr, R., Tratnyek, P.G., Bandstra, J.Z., Scherer, M.M., Alowitz, M.J., Bylaska, E.J., 2004. Diversity of contaminant reduction reactions by zerovalent iron: role of the reductate. Environm. Sci. Technol. 38, 139–147.
Morrison, S.J., Carpenter, C.E., Metzler, D.R., Bartlett, T.R., Morris, S.A., 2002. Desing and performance of a Permeable Reactive Barrier for containment of uranium, arsenic, selenium, vanadium, molybdenum and nitrate at Monticello, Utah. In: Naftz, D.L., Morrison, S.J., Fuller, C.C., Davis, J.A. (Eds.), Handbook of groundwater remediation using Permeable Reactive Barriers. Applications to radionuclides, trace Metals, and nutrients. Academic Press, New York, pp. 371–399.
O'Hannesin, S.F., Gillham, R.W., 1998. Long-term performance of an in situ "iron wall" for remediation of VOCs. Ground Water 36, 164–170.
Phillips, D.H., 2010. Permeable reactive barriers: a sustainable technology for cleaning contaminated groundwater in developing countries. Desalination 251, 352–359.
Rajagopal, B., LeGall, J., 1989. Utilization of cathodic hydrogen by hydrogen oxidizing bacteria. Appl. Microbiol. Biotechnol. 31, 406–412.
Reardon, E.J., 1995. Anaerobic corrosion of granular iron: measurement and interpretation of hydrogen evolution rates. Environ. Sci. Technol. 29, 2936–3294.
Ritter, K., Odziemskowski, M.S., Gillham, R.W., 2002. An in situ study of the role of surface films on granular iron in the permeable iron wall technology. J. Contam. Hydrol. 55, 87–111.
Rivett, M.O., Buss, S.R., Morgan, P., Smith, J.W.N., Bemment, C.D., 2008. Nitrate attenuation in groundwater: a review of biogeochemical controlling processes. Water Res. 42, 4214–4232.
Rodríguez-Maroto, J.M., García-Herruzo, F., García-Rubio, A., Gómez-Lahoz, C., Vereda-Alonso, C., 2009. Kinetics of the chemical reduction of nitrate by zero-valent iron. Chemosphere 74, 804–809.
Ryabenko, E., Altabet, M.A., Wallace, D.W.R., 2009. Effect of chloride on the chemical conversion of nitrate to nitrous oxide for $\delta^{15}N$ analysis. Limnol. Oceanogr. 7, 545–552.
Shin, K., Cha, D.K., 2008. Microbial reduction of nitrate in the presence of nanoscale zero-valent iron. Chemosphere 72, 257–262.
Sigman, D.M., Granger, J., DiFiore, P.J., Lehmann, M.M., Ho, R., Cane, G., van Geen, A., 2005. Coupled nitrogen and oxygen isotope measurements of nitrate along the eastern North Pacific margin. Global Biogeochem, Cy, pp. 19.
Slater, G.F., Lollar, B.S., King, A., O'Hannesin, S., 2002. Isotopic fractionation during reductive dechlorination of trichloroethene by zero-valent iron: influence of surface treatment. Chemosphere 49, 587–596.
Smith, R.L., Kent, D.B., Repert, D.A., Böhlke, J.K., 2017. Anoxic nitrate reduction coupled with iron oxidation and attenuation of dissolved arsenic and phosphate in a sand and gravel aquifer. Geochim. Cosmochim. Ac. 196, 102–120.
Su, C., Puls, R.W., 2004. Significance of iron (II, III) hydroxycarbonate green rust in arsenic remediation using zero valent iron in laboratory column test. Environ. Sci. Technol. 38, 5224–5231.
Suzuki, T., Moribe, M., Oyama, Y., Niinaem, M., 2012. Mechanism of nitrate reduction by zero-valent iron: equilibrium and kinetics studies. Chem. Engineer. J. 183, 271–277.
Till, B.A., Weathers, J.L., Alvarez, J.J.P., 1998. Fe(0)-Supported autotrophic denitrification. Environ. Sci. Technol. 32, 634–639.
Torrentó, C., Cama, J., Urmeneta, J., Otero, N., Soler, A., 2010. Denitrification of groundwater with pyrite and *Thiobacillus denitrificans*. Chem. Geol. 278, 80–91.
Torrentó, C., Palau, J., Rodríguez-Fernández, D., Heckel, B., Meyer, A., Domènech, C., Rosell, M., Soler, A., Elsner, M., Hunkeler, D., 2017. Carbon and chlorine isotope fractionation patterns associated with different engineered chloroform transformation reactions. Environ. Sci. Technol. 51, 6174–6184.
Toyoda, S., Mutobe, H., Yamagishi, H., Yoshida, N., Tanji, Y., 2005. Fractionation of N_2O isotopomers during production by denitrifier. Soil Biol. Biochem. 37, 1535–1545.
Tratnyek, P.G., Scherer, M.M., Johnson, T.L., Matheson, L.J., 2003. Permeable reactive barriers of iron and other zero-valent metals. In: Tarr, M.A. (Ed.), Chemical degradation methods for wastes and pollutants: Environmental and industrial applications. CRC Press, pp. 371–422.
U.S. EPA (2002). Field Applications of In Situ Remediation Technologies: Permeable Reactive Barriers. U.S. Environmental Protection Agency, Office of Solid Waste and Emergency Response, Washington, DC.
Van Breukelen, B.M., 2007. Extending the Rayleigh equation to allow competing isotope fractionating pathways to improve quantification of biodegradation. Environ. Sci. Technol. 41, 4004–4010.
Vitòria, L., Otero, N., Canals, A., Soler, A., 2004. Fertilizer characterization: isotopic data (N, S, O, C and Sr). Environ. Sci. Technol. 38, 3254–3262.
Westerhoff, P., James, J., 2003. Nitrate removal in zero-valent iron packed columns. Water Res. 37, 1818–1830.
Wilkin, R.T., Acree, S.D., Ross, R.R., Puls, R.W., Lee, T.R., Woods, L.L., 2014. Fifteen-year assessment of a permeable reactive barrier for treatment of chromate and trichloroethylene in groundwater. Sci. Total Environ. 468–469, 186–194.
Wunderlich, A., Meckenstock, R., Einsiedl, F., 2012. Effect of different carbon substrates on nitrate stable isotope fractionation during microbial denitrification. Environ. Sci. Technol. 46, 4861–4868.
Wunderlich, A., Meckenstock, R.U., Einsiedl, F., 2013. A mixture of nitrite-oxidizing and denitrifying microorganisms affects the $\delta^{18}O$ of dissolved nitrate during anaerobic microbial denitrification depending on the $\delta^{18}O$ of ambient water. Geochim. Cosmochim. Ac. 119, 31–45.
Xu, C., Wang, X., An, Y., Yue, J., Zhang, R., 2018. Potential electron donor for nanoiron supported hydrogenotrophic denitrification: H_2 gas, Fe0, ferrous oxides, Fe^{2+} (aq), or F^{e2+} (ad)? Chemosphere 202, 644–650.
Xue, D., Botte, J., De Baets, B., Accoe, F., Nestler, A., Taylor, P., Van Cleemput, O., Berglund, M., Boeckkx, P., 2009. Present limitations and future prospects of stable isotopes methods for nitrate source identification in surface and groundwater. Water Res. 43, 1159–1170.
Yabusaki, S., Cantrell, K., Sass, B., Steefel, C., 2001. Multicomponent reactive transport in an in situ zero-valent iron cell. Environm. Sci. Technol. 35, 1493–1503.
Yang, S.-C., Lei, M., Chen, T.-B., Li, X.-Y., Liang, Q., Ma, C., 2010. Application of zerovalent iron (Fe(0)) to enhance degradation of HCHs and DDX in soil from a former organochlorine pesticides manufacturing plant. Chemosphere 79, 727–732.
Yang, G.C.C., Lee, H.L., 2005. Chemical reduction of nitrate by nanosized iron: kinetics and pathways. Water Res. 39, 884–894.
Zhang, Y., Douglas, G.B., Pu, L., Zhao, Q., Tang, Y., Xu, W., Luo, B., Hong, W., Cui, L., Ye, Z., 2017. Zero-valent iron-facilitated reduction of nitrate: chemical kinetics and reaction pathways. Sci. Total Environm. 598, 1140–1150.
Zhang, Y., Douglas, G.B., Kaksonen, A.H., Cui, L., Ye, Z., 2019. Microbial reduction of nitrate in the presence of zero-valent iron. Sci. Total Environm. 646, 1195–1203.